

Hydro-meteorological influences and multimodal suspended particle size distributions in the Belgian nearshore area*

Michael Fettweis¹, Matthias Baeye², Byung Joon Lee³, Peihung Chen⁴, Jason C.S. Yu⁴

¹*Royal Belgian Institute of Natural Science, Management Unit of the North Sea Mathematical Models, Gulledele 100, 1200 Brussels, Belgium*

²*Ghent University, Renard Centre of Marine Geology, Krijgslaan 281 (S8), 9000 Gent, Belgium*

³*Katholieke Universiteit Leuven, Hydraulics Laboratory, Kasteelpark Arenberg 40, 3001 Heverlee, Belgium*

⁴*National Sun Yat-Sen University, Department of Marine Environment and Engineering, Lien-Hai Road 70, 80424 Kaohsiung, Taiwan*

*published in *Geo-Marine Letters* (Springer)

M. Baeye helped writing the manuscript, helped interpreting all datasets (hydro-meteorological data, LISST, SPM, altimetry), and made figures 5.2, 5.3, 5.4 and 5.6. Also, the acoustic-optics interpretation in relation to particle composition was realised by M. Baeye; as well as the LISST ensemble-averaging based on subtidal flow direction.

Abstract

Suspended particulate matter (SPM) concentration and particle size distribution (PSD) were assessed in a coastal turbidity maximum area (southern North Sea) during a composite period of 37 days in January–April 2008. PSDs were measured with a LISST 100X and classified using entropy analysis in terms of subtidal alongshore flow. The PSDs during tide-dominated conditions showed distinct multimodal behaviour due to flocculation, revealing that the building blocks of flocs consist of primary particles ($<3\ \mu\text{m}$) and flocculi ($15\ \mu\text{m}$). Flocculi comprise clusters of clay minerals, whereas primary particles have various compositions (calcite, clays). The PSDs during storms with a NE-directed alongshore subtidal current (NE storms, Case NEW) are typically unimodal and characterised by mainly granular material (silt, sand) re-suspended from the seabed. During storms with a SW-directed alongshore subtidal current (SW storms, Case SWW), by contrast, mainly flocculated material can be identified in the PSDs. The findings emphasise the importance of wind-induced advection, alongshore subtidal flow and high-concentrated mud suspensions (HCMSs) as regulating mechanisms of SPM concentration, as well as other SPM characteristics (cohesiveness or composition of mixed sediment particles) and size distribution in a high-turbidity area. The direction of subtidal alongshore flow during SW storm events results in an increase in cohesive SPM concentration, HCMS formation, and the armouring of sand; by contrast, there is a decrease in cohesive SPM concentration, no HCMS formation, and an increase in sand and silt in suspension during NE storms.

Keywords: Suspended particulate matter; particle size distribution; statistical handling; coastal turbidity maximum; wind impact; seabed variations

5.1. Introduction

Knowledge of the size distribution of suspended particulate matter (SPM) is needed to understand and predict sediment dynamics (Eisma 1986, van Leussen 1994, Curran et al. 2007, Mikkelsen et al. 2007, Winter et al. 2007, Bowers et al. 2009, Lee et al. 2011). Natural SPM comprises many different substances with time- and site-specific concentrations and can be subdivided into inorganic and organic fractions. The inorganic fraction consists mainly of clay minerals as well as carbonates and other non-cohesive minerals (Berlamont et al. 1993, Fettweis 2008); the organic fraction of SPM is prevalently made of micro-organisms and their metabolic products, as well as the remains of dead organisms and faecal pellets (Mari and Burd 1998, Hamm 2002, Bhaskar et al. 2005). Sediments in coastal areas generally consist of sand and mud. The mud-sand ratio influences the transition between cohesive and non-cohesive behaviour, and has a major influence on erosion, SPM concentration, SPM composition and benthic ecological properties (Williamson and Torfs 1996, Panagiotopoulos et al. 1997, van Ledden et al. 2004). In such areas, SPM reflects the bed composition and may consist of a mixture of cohesive and non-cohesive mineral particles (Manning et al. 2010). Close to a sandy seabed, SPM is likely to also contain re-suspended mineral grains, whereas higher in the water column or in muddy environments SPM occurs typically in the form of flocs composed of aggregates of mainly clay minerals, organic matter and water. Mud and sand can be deposited as alternating layers when mud and sand settle either separately from independent suspension or simultaneously. The latter implies segregation due to settling of sand grains through the non-consolidated mud layer (van Ledden et al. 2004).

Flocs vary in size on short time-scales (ebb-flood), as they are formed by collisions due to differential settling of smaller particles with cohesive properties in low-turbulence regimes, and are ruptured by shear in high-turbulence regimes (Lick et al. 1993, van Leussen 1994, Winterwerp 1998). With increasing turbulent shear, breakage of flocs generates smaller particles/flocs but re-suspension of bigger deposited minerals can generate larger particles and flocs in suspension. SPM is therefore likely to have a multimodal particle size distribution (Mikkelsen et al. 2007, Mietta et al. 2010, Lee et al. 2011, Verney et al. 2011), which reflects the fast temporal changes in floc sizes due to variation in turbulent shear as well as the overlapping distributions of flocs and mineral grains in mixed sediment environments under strongly varying shear stresses.

Under laboratory conditions, Manning et al. (2010) have shown that flocculation influences the deposition and settling of sand-mud mixtures. Little data are, however, available that deal with re-suspension of sand, mud and sand-mud mixtures in natural environments. The aim of this work is therefore to present in-situ measurements in an area with mixed bed sediments and to examine the influence of tides, wind and wave effects on the particle size distributions (PSDs) of flocs and granular particles. Furthermore, the potential for mud and sand fractions to occur simultaneously in suspension is discussed, as this can contribute to knowledge on the long-term evolution of a system, notably in terms of conceptual and mathematical models. Understanding of sediment mobility in such environments requires the use of multi-parametric observations supported by mathematical methods. The observations should account for the mutual interaction of sand and mud in suspension as a function of bed armouring, sheltering and exposure effects, erosion and re-suspension, and flocculation dynamics (Wiberg et al. 1994, Wallbridge et al. 1999, Wu et al. 2003). The fragility of flocs makes them difficult to sample, and measurements of floc properties should rely on high-resolution in-situ techniques employing, for example, LISST, floc cameras and holographic cameras (van Leussen 1994, Agrawal and Pottsmith 2000, Manning et al. 2006, Mikkelsen et al. 2006, Benson and French 2007, Graham and Nimmo-Smith 2010).

With this scope in mind, in-situ measurements of SPM concentration, PSDs, and also of currents were carried out in Belgian coastal waters (southern North Sea) by means of optical and acoustical sensors. PSDs provide essential information on floc and particle dynamics, as emphasised by Mikkelsen et al. (2006). In the present study, statistical methods (entropy analysis, fitting of PSDs with summed log-normal functions) and ensemble-averaging have therefore been applied to classify PSDs and to establish links with the underlying processes. Similar measuring approaches (e.g. Fugate and

Friedrichs 2002, Thorne and Hanes 2002, Voulgaris and Meyers 2004, Hoitink and Hoekstra 2005), statistical methods (Jonasz and Fournier 1996, Mikkelsen et al. 2007) and averaging (Murphy and Voulgaris 2006) have been successfully adopted in various marine environments.

5.2. Study site

Measurements were carried out in the Belgian nearshore zone (Fig. 5.1) in the southern bight of the North Sea, characterised by bottom sediments varying from pure sand to pure mud (Verfaillie et al. 2006) and by highly turbid waters. Nearshore SPM concentration ranges between $0.02\text{--}0.07\text{ g l}^{-1}$ and reaches 0.1 to $>3\text{ g l}^{-1}$ near the bed; lower values ($<0.01\text{ g l}^{-1}$) occur offshore (Fettweis et al. 2010).

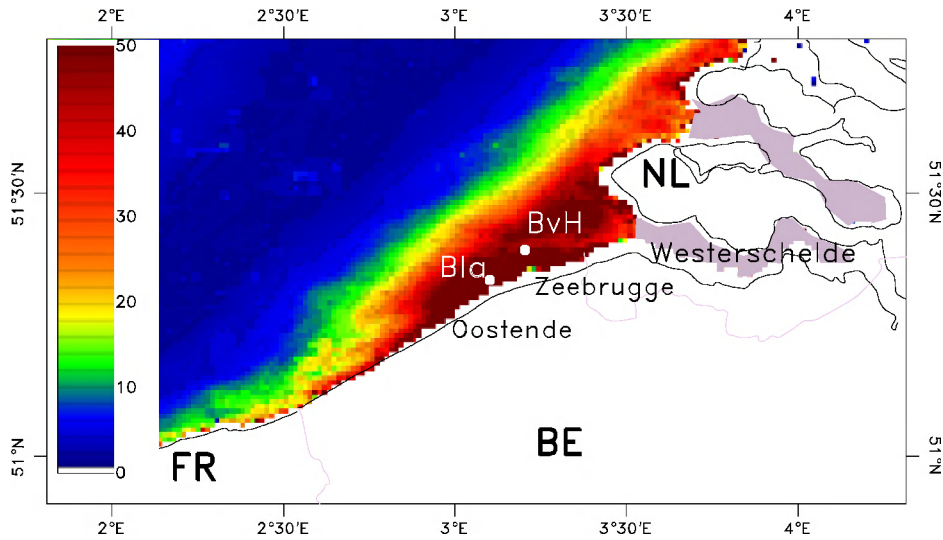


Figure 5.1 Map of the Belgian coastal area (southern North Sea), showing yearly averaged surface SPM concentration (mg dry wt l^{-1}) derived from moderate resolution imaging spectroradiometer (MODIS) images of 2002–2009 (extracted from Nechad et al. 2010), the tripod measurement station at Blankenberge (Bla) and the wave measurement station at Bol van Heist (BvH); coordinates are in $^{\circ}\text{N}$ latitude and $^{\circ}\text{E}$ longitude

The tidal regime is semi-diurnal, and the mean tidal range at Zeebrugge is 4.3 and 2.8 m at spring and neap tide, respectively. The tidal current ellipses are elongated in the nearshore area and become gradually more semi-circular towards the offshore. The current velocities near Zeebrugge (nearshore) vary from $0.2\text{--}1.5\text{ m s}^{-1}$ during spring tide and $0.2\text{--}0.6\text{ m s}^{-1}$ during neap tide. Ebb currents are directed towards the southwest and flood currents towards the northeast.

South-westerly winds dominate the overall wind climate, followed by winds from the NE sector. Maximum wind speeds coincide with the south-westerly winds; nevertheless, the highest waves are generated under north-westerly winds. Salinity varies between 28 and 34 PSU in the coastal zone, due to wind-induced advection of water masses and river discharge (Lacroix et al. 2004, Fettweis et al. 2010).

The effect of hydro-meteorological forcing (tide- and wind-induced flows) on SPM transport and the formation of high-concentrated mud suspensions (HCMSs) has been investigated by Baeye et al. (2011) for the Belgian nearshore area. They report that winds blowing from the N-NE increase and those (however no storm winds) from the SW decrease the overall SPM concentration at the measurement site. The latter is related to advection of less turbid English Channel water, inducing a shift of the turbidity maximum towards the NE and the Westerscheldt estuary. Under these conditions, marine mud is imported into the estuary. Under protracted NE winds,

HCMSs are formed and can persist during several tidal cycles. The measurement station Blankenberge is situated about 5 km SW of the port of Zeebrugge, in the eastern part of a shoreface-connected sand ridge (Wenduine Bank) at about 1 km from the shore (Fig. 5.1). The water depth varies between about 6 and 10 m at this location. Sediment samples near Blankenberge show variable sediment characteristics with a median grain size of about 150 μm .

5.3. Materials and methods

5.3.1. Instrumentation and deployment

Data were collected between January and April 2008 over a composite period of 37 days, using a tripod to measure currents, salinity as well as SPM concentration and PSD (see Table 5.1, and figure captions for dates). The instrumentation suite consisted of a 5 MHz SonTek Acoustic Doppler Velocimeter (ADV Ocean-Hydra), a 3 MHz SonTek Acoustic Doppler Profiler (ADP), two D&A optical backscatter point sensors (OBSs), a Sea-bird SBE37 CT and a Sequoia Scientific LISST (laser in-situ scattering and transmissometry) 100 X type C. All data (except LISST) were stored in two SonTek Hydra data logging systems.

The LISST was mounted at 2 meters above the bed (hereafter referred to as mab) and the OBSs at 0.2 and 2 mab. ADV velocities were measured at 0.2 mab, while the ADP profiler was attached at 2.3 mab and down-looking, measuring current and acoustic intensity profiles with a bin resolution of 0.25 m. Mean values were obtained every 10 minutes for the OBS, LISST and ADV, while the ADP was set to record a profile every 1 minute; subsequent averaging was performed at a 10-minute interval to match the sampling interval of the other sensors. The long deployments ensured accurate assessments of conditions over complete neap and spring tides, and included a variety of meteorological events.

Table 5.1 Modal size (μm) and volumetric fractions (%) of primary particles (PP), flocculi, microflocs and macroflocs for the entropy groups of the two deployments (cf. Fig. 5.5). Mode 1 (PP) and mode 2 (flocculi) have a fixed size of 3 and 15 μm respectively

	PP	Flocculi	Microflocs	Macroflocs
Group 1	6%	43%	46 μm , 47%	230 μm , 4%
Group 2	2%	25%	58 μm , 68%,	271 μm , 5%
Group 3	1%	16%	87 μm , 80%	360 μm , 3%
Group 4	1%	15%	119 μm , 69%	339 μm , 16%

5.3.2. SPM concentration, HCMSs and turbulence

The OBS and ADP backscattered signals were used to estimate SPM concentration. OBS voltage readings were converted into SPM concentration by calibration against filtered water samples during several field campaigns (Fettweis et al. 2006). A linear relationship was assumed between all OBS signals and SPM concentrations from filtration. After conversion to decibels, the ADP backscattered acoustic signal strength was corrected for geometric spreading and water attenuation. Furthermore, an iterative approach (Kim et al. 2004) was used to correct for sediment attenuation. The highest OBS-derived SPM concentration estimates were used to empirically calibrate the ADP's first bin. As variations in SPM composition and size were not taken into account, the ADP backscatter signal was calibrated in terms of 'average' SPM. Limitations associated with optical and acoustic instruments have been addressed by Thorne et al. (1991), Hamilton et al. (1998), Bunt et al. (1999), Fugate and Friedrichs (2002), Voulgaris and Meyers (2004) and Downing (2006). In general, acoustic

backscattering is affected by sediment type, size and composition. All these parameters are difficult to quantify by single-frequency backscatter sensors (Hamilton et al. 1998). OBSs have primarily been designed to be most sensitive to SPM concentration; size effects are an order of magnitude lower than those of concentration, and flocculation effects are even smaller (Downing 2006). Compared to optical devices, acoustic devices are more sensitive to coarser grain sizes and thus produce better estimates of the mass concentration of the coarser granular fraction. Briefly, when SPM composition changes from very fine material to silt- or sand-sized grains without changes in concentration, then the SPM concentration derived from acoustic and optical backscattering will differ. An ADP calibrated for fine material will have a stronger backscattering and, thus, it produces an apparently higher concentration when the SPM becomes coarser. By contrast, under these circumstances the optical backscatter signal will decrease, resulting in an apparent decrease in SPM concentration.

Besides the time-series of current velocities and acoustic amplitude, the ADP was also configured to measure and store the distance between sensor and seabed (Baeye et al. 2011). The altimetry of the ADP was used to detect variation in bed level, and also for the identification of deposition and re-suspension of fine-grained sediments. For the study site, decreasing distance between the probe and the bed boundary can correspond to the presence of HCMs acting as an acoustic reflector.

The high-frequency ADV measurements (measuring rate of 25 Hz) were used to decompose the velocity in terms of a mean and a fluctuating part. The variance of velocity fluctuations served to calculate the turbulent kinetic energy (TKE), this being a measure of turbulence intensity (Pope et al. 2006).

5.3.3. Classification of PSDs

Two methods for the classification of particle size spectra were applied. The one uses the flow data to separate the LISST records into different groups corresponding to different hydrodynamic forcing. The collected time-series were filtered for the tidal signal using a low-pass filter for periods less than 33 h, and decomposed into along- and cross-shore components. The alongshore low-pass flow served to characterise the tidal cycle in terms of wind-driven flow. Three cases were identified, one corresponding to pure tidal flow (Case 0) and two to periods with significant influence of wind-driven flows: case SW (or Case SWW cf. Chapter 2) has winds from the NW-NE resulting in residual alongshore currents directed towards the SW; case NE (or Case NEW cf. Chapter 2) has winds from the SW and residual alongshore currents directed towards the NE. Moreover, each tidal cycle was classified as neap or spring depending on the particular tidal range. This classification has resulted in a total of six categories of tidal cycles, where each category represents both tidal and wind forcing. Tidal cycles from each category were ensemble-averaged to create a representative tidal cycle for each case (cf. Murphy and Voulgaris 2006, Baeye et al. 2011 for a more detailed description of the method).

The other method of classification entails entropy analysis to evaluate the randomness of an event (such as a particle size distribution) and to assign the event to a group with similar characteristics. Applied to PSDs, entropy analysis allows grouping the size spectra without assumptions about the shape of the spectra and is therefore suited for analysis of unimodal, bimodal as well as multimodal distributions (Woolfe et al. 1998). Entropy analysis has been successfully applied to grain size distributions from sedimentary deposits (Forrest and Clarke 1989, Woolfe and Michibayashi 1995, Woolfe et al. 1998, Orpin and Kostylev 2006) and to LISST particle size distributions of suspended matter (Mikkelsen et al. 2007, Krivtsov et al. 2011). Our analysis was carried out with the FORTRAN routine of Johnston and Semple (1983) extended with a module to calculate the optimal number of groups using the Calinski-Harabasz pseudo F-statistic (Orpin and Kostylev 2006, Stewart et al. 2009). The results are presented as an averaged and normalized PSD for each group.

5.3.4. Multimodal log-normal distribution function

Mathematical functions such as summed log-normal distribution functions can be used to describe PSDs. This approach was applied to decompose the averaged and

normalized PSDs from entropy analysis into a sum of four log-normal functions, in order to quantify the volumetric fraction of primary particles, flocculi, micro- and macro-flocs. This four-level ordered structure results from flocculation of clay minerals, as reported by van Leussen (1994). The multimodal log-normal distribution function can then be written as an integrated distribution function of four log-normal distribution functions (Whitby 1978, Jonasz and Fournier 1996, Sun et al. 2002,

$$\text{Hussein et al. 2005): } \frac{dW}{dD} = \sum_{i=1}^4 \frac{\overline{W}_i}{\sqrt{2\pi\ln(\sigma_i)}} \exp \left[-\frac{1}{2} \left(\frac{\ln(D/\overline{D}_i)}{\ln(\sigma_i)} \right)^2 \right]$$

where D is the particle diameter, W the volume concentration, \overline{D}_i the geometric mean diameter, σ_i the geometrical standard deviation, and \overline{W}_i the volumetric fraction of an i th unimodal PSD. The DistFit™ software (Chimera Technologies, Forest Lake MN, USA), which has been widely employed in analyzing aerosol particles, was used to generate the best fits, defined as the minimum errors between fitted and measured PSDs (Whitby 1978, Hussein et al. 2005). For two modal peaks, fixed sizes of 3 μm (lowest size class of the LISST) and 15 μm were chosen; the modal peaks of the bigger fractions were variable (15–200 and 200–500 μm). The standard deviations were allowed to vary between 1 and 2.5. The choice of parameters is based on assumptions and experiences (cf. Makela et al. 2000, Lee et al. 2011).

5.4. Results

5.4.1. Time-series

The SPM concentration derived from the ADP (2 mab) and OBS (2 and 0.2 mab), the median particle size derived from the LISST, the along- and cross-shore subtidal flow, and the seabed altimetry derived from the ADP are presented in Fig. 5.2 and 6.3 for the two deployments. Note that the alongshore flow is positive when it is directed towards the NE and negative towards the SW. Positive cross-shore flow is directed towards the shore.

Two storms were registered during the January–February 2008 deployment. The first occurred on days 30.5 to 32.5 (1–2 February) and had a significant wave height (H_s) of up to 2.8 m. The second was on days 35–37 ($H_s=1.5$ m; see Fig. 5.2). The wind direction during both storm events was variable from the SW to the W and NW at times of peak wave heights. The wind during and before these time periods was generally blowing from the SW–W, resulting in a positive subtidal alongshore flow; these are therefore called NE-ward storms (NE storms). During the rest of the deployment, the significant wave heights were lower ($H_s<1.5$ m) and the wind blowing mainly from the SW and W.

SPM concentration at 2 mab (OBS) varied between 0.01 and 1.5 g l^{-1} during the calmer periods, with distinct neap–spring tidal variations. The SPM concentration at both 0.2 and 2 mab (OBS) decreased to less than 0.1 g l^{-1} during the first storm (days 30.5–32.5). The SPM concentration derived from the ADP was generally lower than that of the OBS (2 mab), except during the onset of the storms when the 2-mab OBS signal decreased, whereas the backscattered ADP signal increased. The SPM concentration from the ADP during the first storm is significantly correlated with the wave height, and the tidal signal is hardly distinguishable.

The variations in median particle size (D50: 20 to >180 μm) during calm meteorological conditions were typically associated with the tidal current variations. Largest floc sizes occurred around slack water and smallest ones during maximum currents. The LISST data show significantly different median particle sizes and particle size variations during the storm periods.

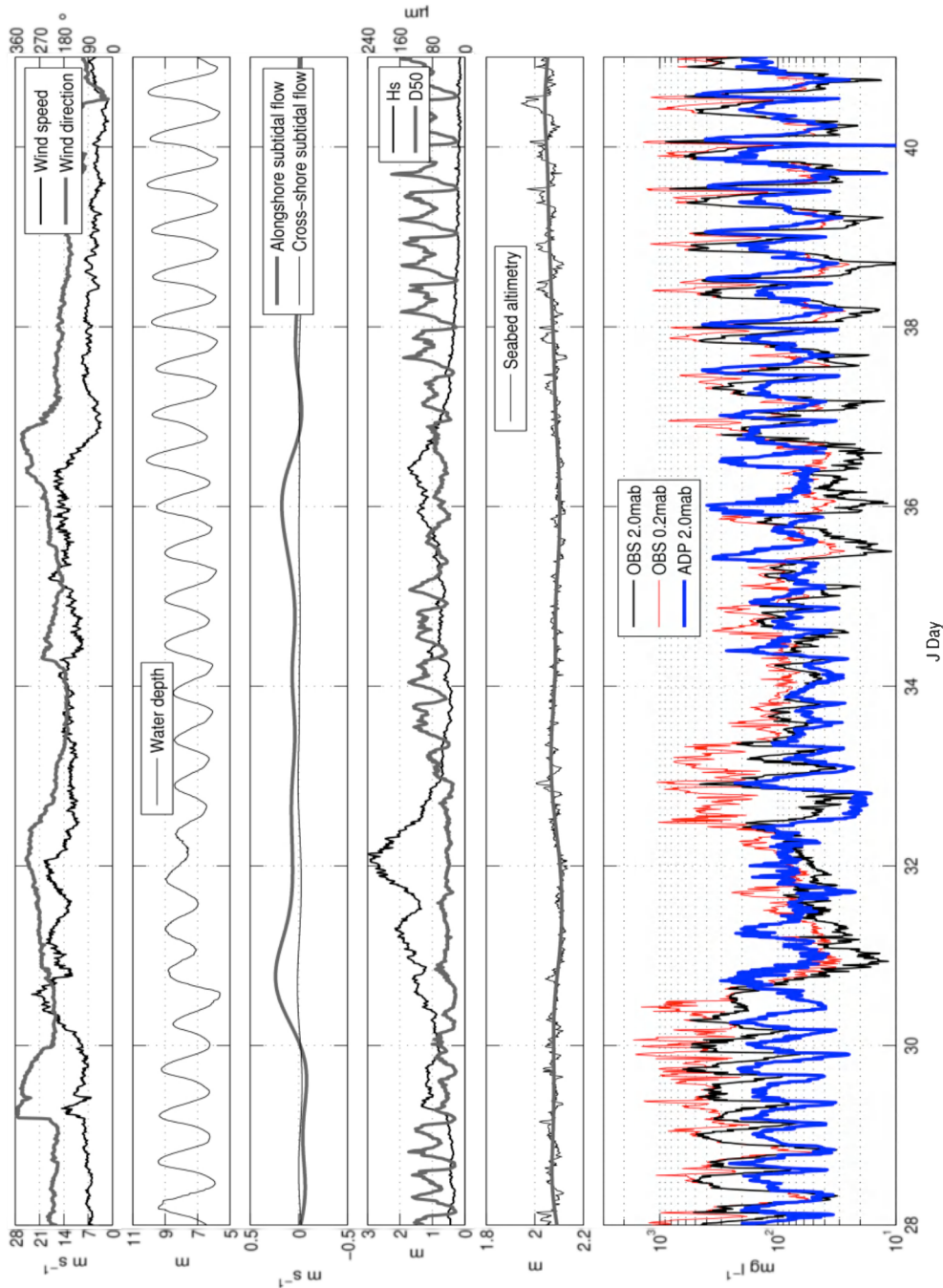


Figure 5.2 January–February 2008 deployment (28/01 15:38 to 11/02 13:40); time-series of wind velocity and direction (wind from 0°=N, 90°=E, 180°=S, 270°=W) at Bol van Heist; water depth; subtidal alongshore (positive towards the NE, negative towards the SW) and cross-shore flow (positive onshore, negative offshore); significant wave height and D50 of particle size distribution; seabed altimetry; and SPM concentration from OBS (0.2 and 2 mab) and ADP (2 mab)

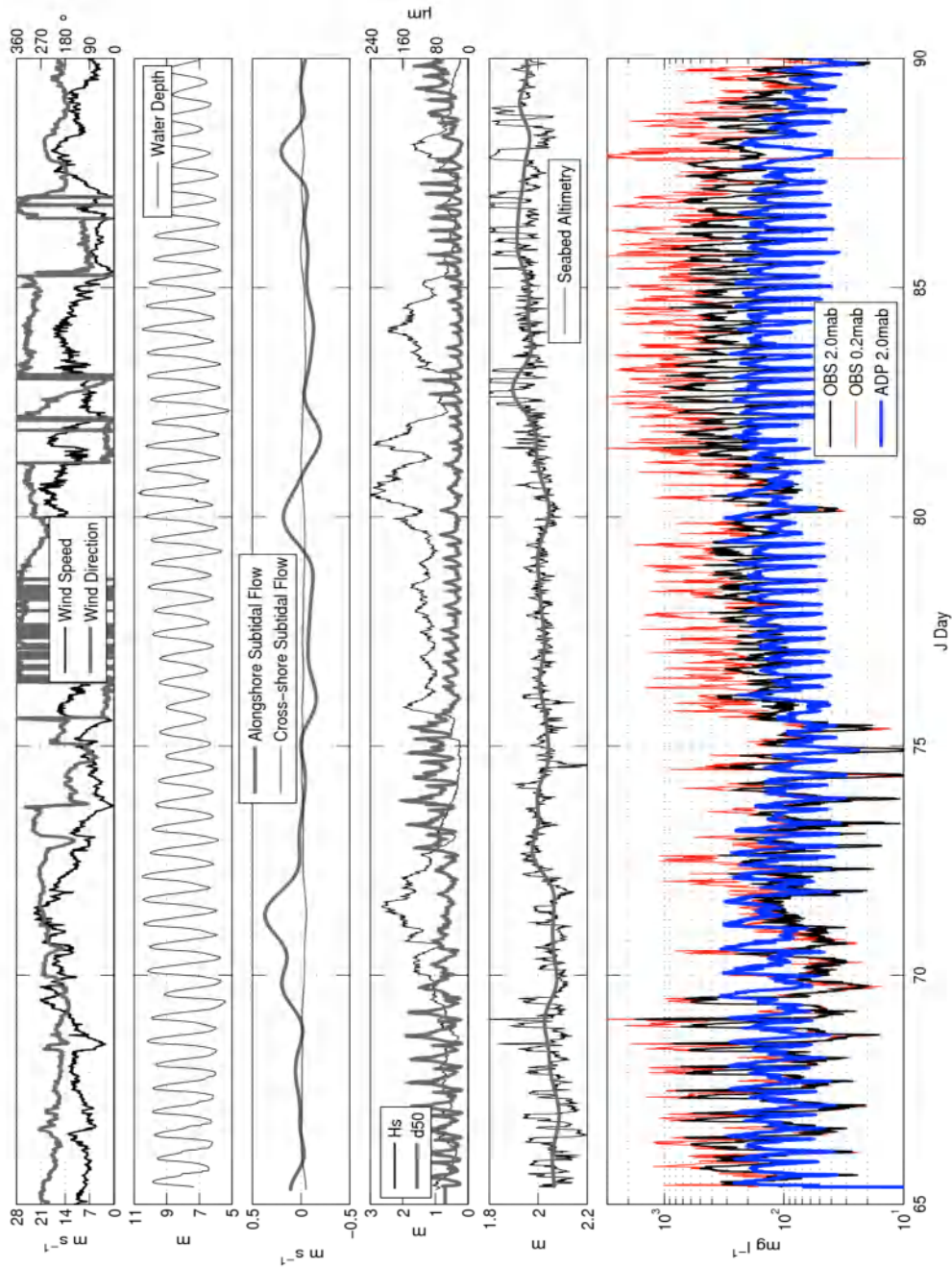


Figure 5.3 March–April 2008 deployment (06/03 09:09 to 08/04 15:29): time-series of wind velocity and direction (wind from $0^\circ=N$, $90^\circ=E$, $180^\circ=S$, $270^\circ=W$) at Bol van Heist; water depth; subtidal alongshore (positive towards the NE, negative towards the SW) and cross-shore flow (positive onshore, negative offshore); significant wave height and D50 of particle size distribution; seabed altimetry; and SPM concentration from OBS (0.2 and 2 mab) and ADP (2 mab)

The maxima of D50 were smaller and the minima bigger than during periods with mainly tidal forcing (D50: 30–60 μm on days 31–32.5, and 45–70 μm on days 35–37). The typical quarter-diurnal tidal signal in D50 has disappeared during the first NE

storm. The distance between the ADP and the seabed (altimetry) increased during both NE storms, and varied as a function of tides from day 38 on, when the weather was calm. The March–April 2008 deployment was characterised by generally stronger winds (see Fig. 5.3). Significant wave heights of up to 2.5 m were recorded between days 70 and 73 (10–13 March) during a period of SW wind turning towards the W. This storm and a short period around days 79–81 (19–21 March) are associated with positive subtidal alongshore flow and are also classified as 'NE storm'. Similar to the first two storms (days 31–32.5 and 35–37, Fig. 5.2), the SPM concentration at 2 mab derived from the OBS was lower than that from the ADP backscattered signal. The SPM concentration at 0.2 mab was also low. The altimetry increased during both NE storms. The next storms were all characterised by northerly wind directions (NE–N–NW). This type of wind direction generates a negative subtidal alongshore flow directed towards the SW and, therefore, these are called SW-ward storms (SW storms). They occurred on days 76–79 (16–19 March) and days 81–85 (23–25 March). The H_s reached values of 2 m (day 76), 3 m (day 81), 2.7 m (day 84) and 1.8 m (day 88).

The SPM concentration (OBS) was high during the whole period, especially around days 81–88, whereas the SPM concentration from the ADP was always lower ($<0.25 \text{ g l}^{-1}$), which is in contrast with the observation made during the NE storms of February and March. The SPM concentration at 0.2 mab reached high values ($>3 \text{ g l}^{-1}$), pointing to the occurrence of an HCMS. The latter is confirmed by the generally lower altimetry (and higher seabed) during the period. The data show also that periods with negative alongshore flows (SW storms) are related with decreasing altimetry; however, lowest altimetry was after the storm. The tidally averaged SPM concentration at 2 mab (OBS) varied between $0.6\text{--}1.0 \text{ g l}^{-1}$ at 2 mab and between $1.6\text{--}3.0 \text{ g l}^{-1}$ at 0.2 mab. The median particle size of the SPM during the SW storms was similar to that of the NE storms; smaller maxima and larger minima ($20\text{--}60 \mu\text{m}$) were observed than during the meteorological calm periods ($15\text{--}150 \mu\text{m}$). However, the median particle size during the NE storms (days 70–73 and day 32) was clearly different from that of the SW storms (days 81–85). The NE storm at the end of the time-series (day 88, 28 March) is different from the previous in the sense that ADP and OBS SPM concentrations show similar behaviour. The storm followed a period with prominent HCMS layers and evidently was too short for the flocs to be transported away from the site.

5.4.2. Classification of PSDs

The PSD groupings according to alongshore currents are shown in Fig. 5.4. As PSDs represent averages of large amounts of data, which show typical behaviour related to prominent hydro-meteorological conditions, the short-term events such as storms are filtered out. Multimodal distributions caused by formation of macroflocs occurred during ebb and were typically associated with case 0 (no wind) and case NE. They are more obvious during high-energy conditions (spring tide). Multi-modality due to the occurrence of a rising tail in the lowest size classes of the LISST or a peak in the distribution around $150 \mu\text{m}$ occurred at peak flood velocity (most obvious for SW spring tide).

Entropy analysis revealed that the optimal number of entropy groups was 4. The averaged PSDs per group are shown in Fig. 5.5, and the corresponding temporal distributions of the groups in Fig. 5.4. In contrast with the grouping based on alongshore currents (Fig. 5.4), the entropy-based grouping involves mathematical and not physical characteristics. Nevertheless, the results show that the entropy groups correspond with specific conditions during a tidal cycle and during storm periods, indicating a transition from unimodal distributions with rising tails in the lowest size classes towards multimodal distributions with gradually higher probabilities of occurrence of macroflocs. The shape of group 1 is convex for the lower size classes and concave for the larger sizes. The shape of the distributions in the next size classes becomes gradually more concave in the lower and more convex in the larger size classes. The different groups of particle size distributions obtained, using the entropy method, have been fitted with a sum of four log-normal functions. The volume fraction and geometric mean of the four modes are presented in Table 5.1 and Fig. 5.7. The finest particles represent 1–6% (primary particles) and 15–43% (floculi) of the volume fraction, the microflocs have modes between $46\text{--}119 \mu\text{m}$ and represent 47–

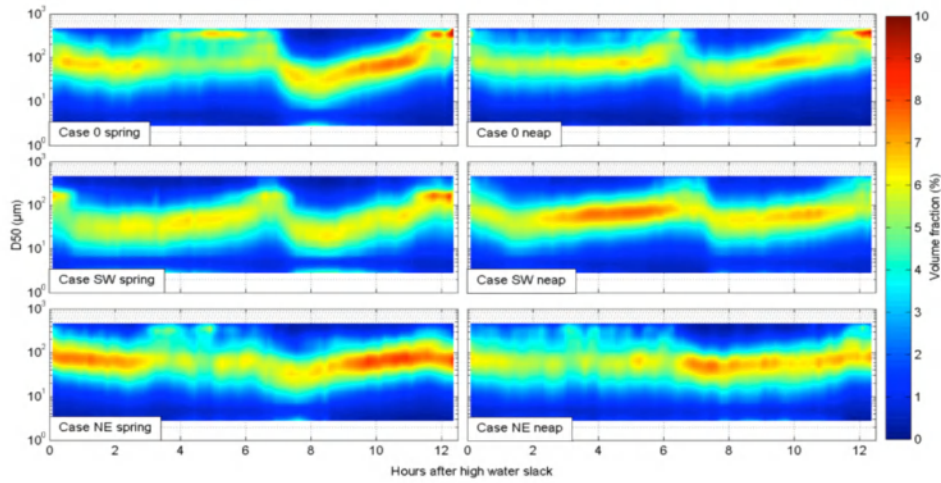


Figure 5.4 Classification of PSD as a function of alongshore subtidal currents: averaged PSD during one tidal cycle at 2 mab for (from top to bottom) case 0 (no wind), case SW (SW-directed alongshore subtidal current) and case NE (NE-directed alongshore subtidal current) at (from left to right) spring and neap tide

80% of the volume fraction, and the macroflocs have a mode of 230–360 μm and a volume fraction varying between 4–16%.

5.5. Discussion

The different entropy groups as well as the low-pass filtered tidal PSDs indicate a transition between bimodal distributions with rising tails in the lowest size classes and multimodal distributions with gradually bigger particle sizes when turbulence decreases. This behaviour is well described in the literature (e.g. Manning et al. 2006; Mikkelsen et al. 2007; Mietta et al. 2010; Verney et al. 2011) and is typically associated with tidal forcing. PSDs during storm conditions or other high-energy conditions (maximum flood currents during spring tide) are different and show unimodal or multimodal distributions. Below some points are discussed in more detail to explain these as a combination of flocculation processes and erosion events of non-cohesive sediments.

5.5.1. Flocculation: primary particles, flocculi, flocs

Several characteristic behaviours of the PSDs were identified by curve fitting analysis. The PSDs have a major modal peak of microflocs and additional peaks, such as a rising tail in the lowest size class (primary particles), and humps of small particles (flocculi) and macroflocs (Fig. 5.7). The data show that the macroflocs in the Belgian nearshore area have a geometric mean between 230–360 μm and the microflocs between 46–119 μm . Significant amounts of macroflocs occur only in group 4. The microfloc population was characterised by a gradual shift of the PSD towards bigger size classes at times of decreasing currents.

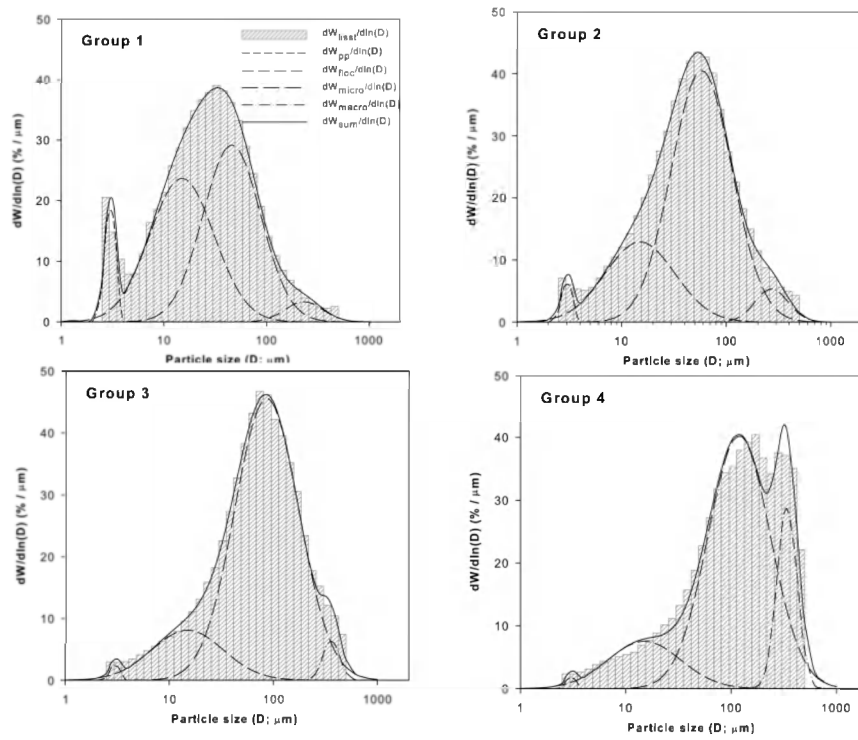


Figure 5.5 January–February and March–April 2008 deployments: averaged PSD for the four entropy groups, $dW_{iss}/d\ln(D)$, together with the fitted sum of the four log-normal functions, $dW/d\ln(D)$

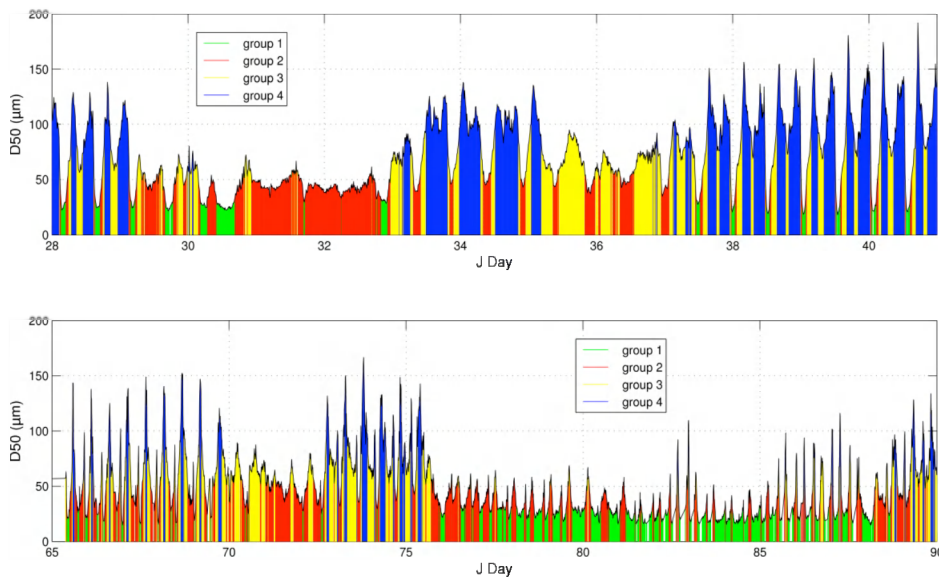


Figure 5.6 January–February and March–April 2008 deployments: temporal distributions of the four entropy groups

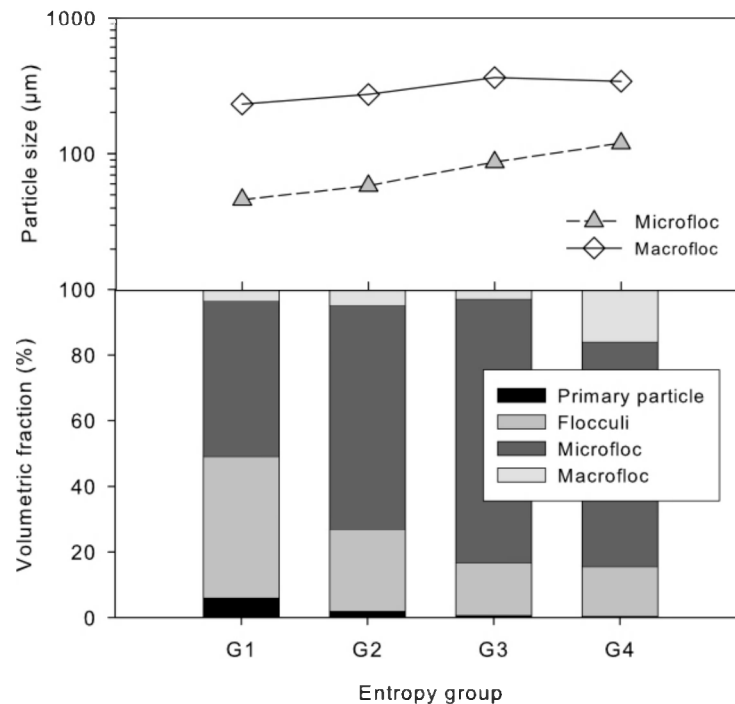


Figure 5.7 Modal sizes and volumetric fractions of primary particles, flocculi, microflocs and macroflocs in the four entropy groups during both deployments

The rising tail in the lowest size classes is due to the presence of particles up to 10 times smaller than the smallest size bin (i.e. 0.25–2.5 μm), as well as the occurrence of non-spherical particles (O.A. Mikkelsen, personal communication). Andrews et al. (2010) report that fine 'out of range' particles affect the entire PSD, with a significant increase in the volume concentration of the first two size classes of the LISST, a decrease in the next size classes and, surprisingly, a small increase in the largest size classes. 'Out of range' particles (<2.5 μm) cause an erroneous size distribution (Andrews et al. 2011). The rising tail in our data corresponds with very fine particles resulting from floc breakage. The curve fitting at the 3 μm mode is thus a relict of the inaccuracy of the LISST instrument for fine particles. The volume fraction calculated for this size distribution should therefore be interpreted as an indication for the presence of very fine particles or primary particles. Pre-treatment of fine sediments is needed in order to measure the grain size of individual clay particles (Huang 1989); this suggests that in marine waters clay minerals occur as clusters (with sizes of 15 μm) of a few crystals, as well as individual crystals. Chang et al. (2007) mention that only the fraction <8 μm (analysed after pre-treatment in the laboratory) is present in flocs. This, together with the fact that the median grain size of the SPM from the study area is about 2 μm (Fettweis 2008), confirms that our flocculi (15 μm) consist of clusters of clay minerals rather than silt-sized particles, which are hardly broken down to primary particles (clay minerals), even under high shear (Mietta 2010). The data show that primary particles of possibly different composition (calcareous particles, clay minerals) and flocculi occur as building blocks of the flocs. This could explain why fractal theory based on a single type of primary particle is not able to accurately describe flocculation (Kranenburg 1994, Fettweis 2008).

The PSDs are dominated by primary particles, flocculi and microflocs at maximum flood velocity, suggesting partially disruption of microflocs into primary particles and flocculi, and nearly complete disappearance of the fragile macroflocs (Fig. 5.4 and 5.7). The fact that macroflocs are still found at high current velocities (entropy groups 1 and 2) can possibly be explained by the occurrence of fine 'out of range' particles, as reported by Andrews et al. (2010); the actual volume concentration of macroflocs during these events is thus probably lower. The TKE as a function of median particle

size (D_{50}) is shown in Fig. 5.8 for different situations. TKE is low during calm weather conditions (Fig. 5.8 a); the fact that a hysteresis relation is observed during ebb and flood indicates that floc size is primarily a function of turbulence and available residence time (Winterwerp 1998). Macroflocs are formed during slack water, when turbulence is low, but also during ebb, when currents are still significant but less so than during flood. The latter suggests that mild turbulence below a threshold favours collision and enhances flocculation. When turbulence becomes too high above the threshold, then flocs are disrupted.

5.5.2. Erosion: mixed sediments in suspension

The rising tail in the finest classes of the entropy spectra is associated with high-energy events (group 1 in Fig. 5.5, 5.6) and indicates floc breakage. It was therefore surprising to see that, during SW storm conditions, only a small rising tail was detected in the finest size classes of the LISST. The PSD was log-normally distributed, almost unimodal, and the main mode

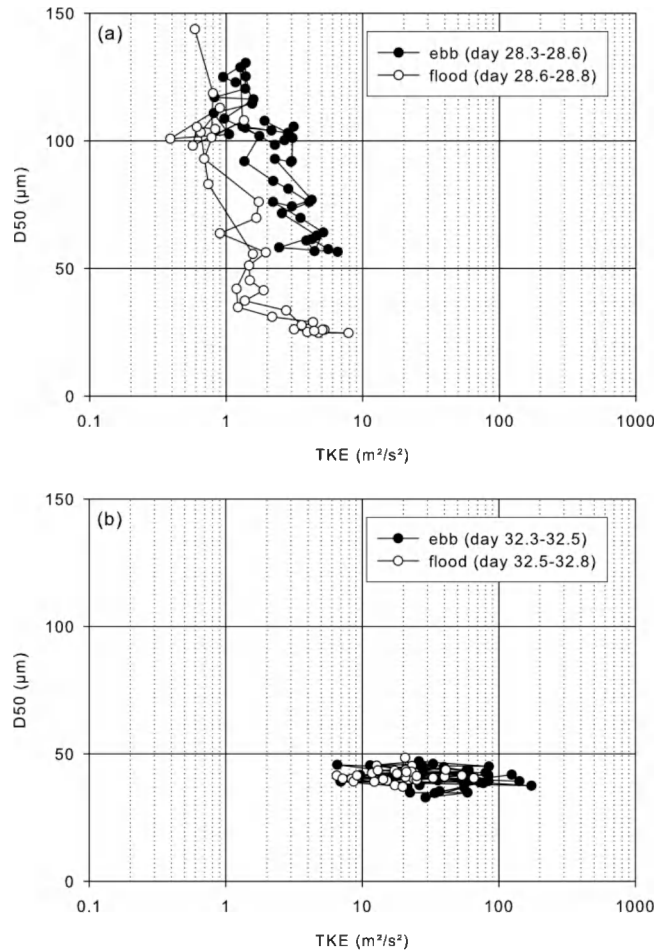


Figure 5.8 Turbulent kinetic energy (TKE) as a function of median particle size: **a** neap tide (day 28), **b** NE storm (day 32)

remained almost constant in size ($D_{50} \approx 50 \mu\text{m}$; see entropy group 2 occurring dominantly around days 32 and 71; Fig. 5.5, 6.6). NE storms were characterised by lower SPM concentrations derived from the OBS than from the ADP at 2 mab (Fig. 5.2, 5.3), suggesting that the composition and size of the SPM has partially changed from

flocculated fine-grained material to silt-sized grains. The latter is confirmed by the distinctly different PSD measured during these events (Fig. 5.5, 5.6), as well as by the observation that TKE has almost no effect on particle size (Fig. 5.8 b, c), in contrast with calm weather (Fig. 5.8 a) and SW storm conditions (Fig. 5.8 d).

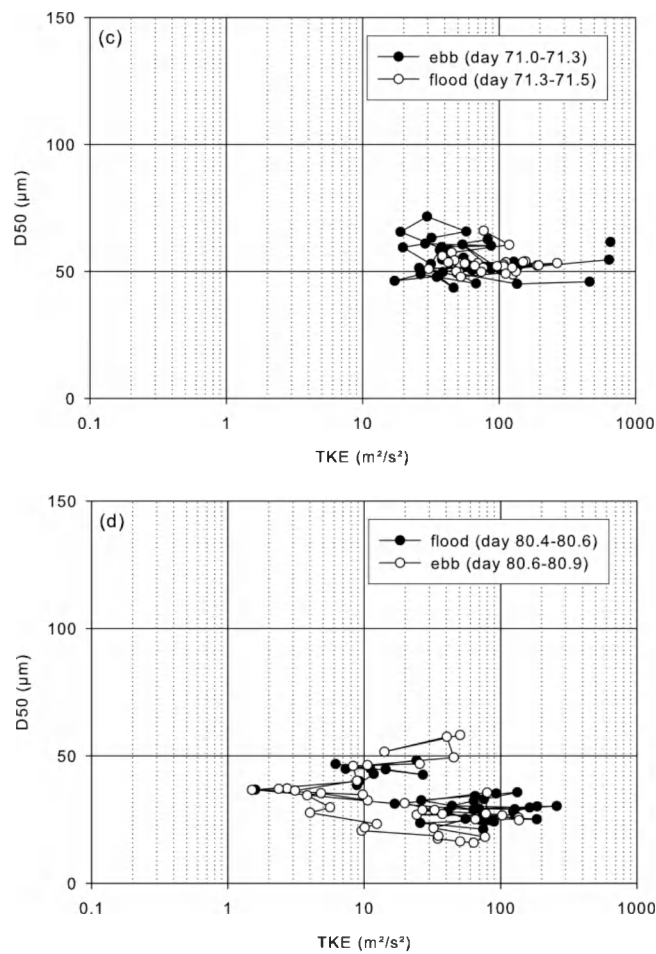


Figure 5.8 (continued) Turbulent kinetic energy (TKE) as a function of median particle size: **c** NE storm (day 71) and **d** SW storm (days 80–81)

Furthermore, the altimetry signal increased, pointing to erosion events and, thus, disappearance of fine-grained material. The low SPM concentration derived from the OBS during the NE storms is thus most probably caused by changes in the size and composition of SPM, explaining the apparent decrease in SPM concentration (Downing 2006). If composition would not have changed, then one would expect an increase in optical backscattering during high-energy events as flocs break up, resulting in an apparent increase in SPM concentration (Agrawal and Traykovski 2001). The fact that, during NE storms, PSDs and acoustical and optical backscatter signals varied differently can be explained only by a decrease in concentration of flocculated material and by changes in the composition of SPM due to wave-induced re-suspension of coarser bed material. Prevailing SW winds enhance NE-directed subtidal flow, which generally results in a decrease in SPM concentration at this site due to advection of low-turbidity, high-salinity water from the English Channel towards the measurement site (Baeye et al. 2011). The latter is confirmed by the increase in salinity observed during this period. The lower concentration of flocs explains the absence of a rising tail

in the PSD spectra (Fig. 5.9 a, b) during the storm, in contrast with the PSDs at times of maximum flood currents.

During SW storms (days 81–85, Fig. 5.3), a different behaviour was observed: SPM concentration derived from the OBS increased, whereas that derived from the ADP did not show significant changes. The PSDs during this storm were mostly characterised by a prominent rising tail in the smallest size classes (see dominance of group 1 in Fig. 5.6 around SW storms, and Fig. 5.9 c, d). The shape of the PSD during the SW storm varied from more convex in the lower size classes and more concave in the bigger sizes towards gradually more concave in the lower size classes and more convex in the higher size classes when currents decreased (see Fig. 5.9 c, d). This is typically associated with flocculation (Mikkelsen et al. 2007).

Compared to NE storms, the higher concentration of flocs observed during SW storms is related to different subtidal alongshore flow directions (see above). The observed increase in SPM concentration in the OBS signal at 0.2 and 2 mab is thus mainly caused by the advection of fine material into the study area. SW storm conditions are often associated with the occurrence of persistent HCMS layers (Fettweis et al. 2010). The latter is confirmed by the higher seabed level derived from ADP altimetry (Fig. 5.3); this is typically associated with HCMS formation, as reported by Baeye et al. (2011). These authors argue that they act as inverse armouring and prevent sand and silt from being eroded. Non-cohesive grains are detected only if the turbulence is high enough to lift the particles up to 2 mab. The seabed consists of sand and silt and is generally not covered by HCMSs during NE storm conditions, as SPM concentrations are generally lower due to the advection of less turbid English Channel water. It is under these conditions that sand and silt dominate the SPM (SW storm, Fig. 5.9 a, b).

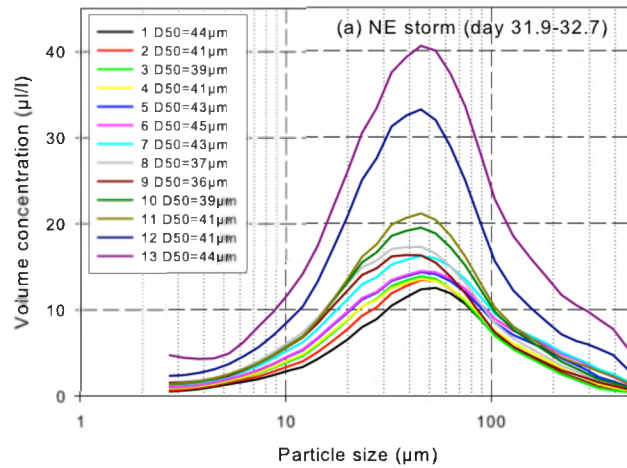


Figure 5.9 Hourly PSD during a tidal cycle for two NE storms (**a**, **b**), and during flood (**c**) and ebb (**d**) for a SW storm

5.5.3. Breaking waves and air bubbles

Air bubbles are inevitably linked with the presence of wind-driven sea waves. Individual bubble clouds are generated by breaking waves and persist for several minutes (Thorpe 1995). The size of bubbles varies strongly and can range between tens of μm up to a few cm (Deane and Stokes 2002); as such, it falls partially into the size range of the LISST. As the measurement site is situated in shallow waters (6 m MLLWS), the occurrence of air bubbles during storms could possibly influence the measurements. At a water depth of 6–10 m, waves start to break if the wave height divided by water depth is bigger than 0.78 (CEM 2003); this occurs for wave heights >4.7 m and indicates that, during the recorded storms when the significant wave heights reached up to 3 m, the waves were only occasionally breaking around low water. It is therefore not very likely that air bubbles significantly influenced the volume concentration and size distribution of SPM.

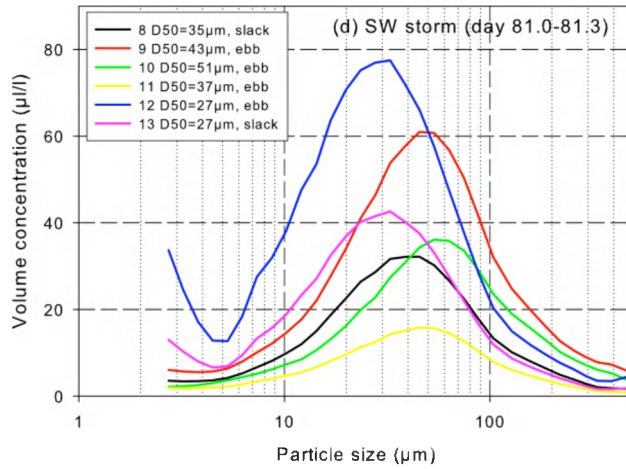
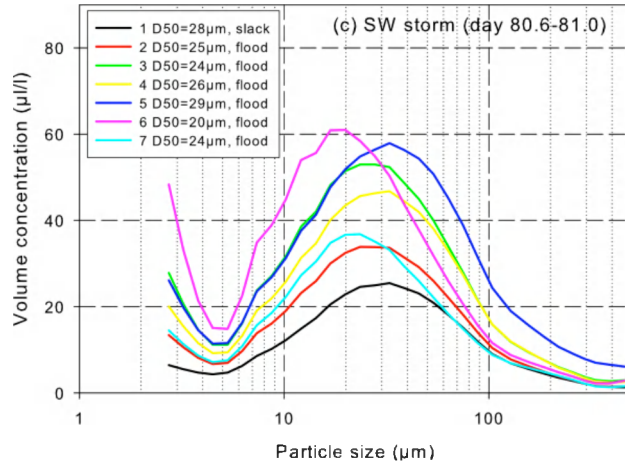
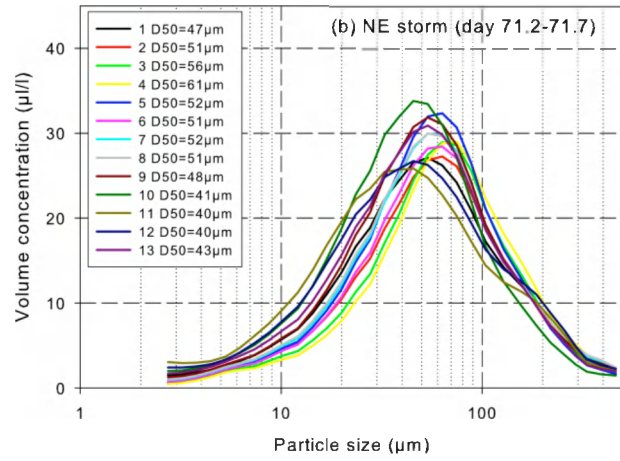


Figure 5.9 (continued) Hourly PSD during a tidal cycle for two NE storms (**a**, **b**), and during flood (**c**) and ebb (**d**) for a SW storm

The findings that two different types of storms with similar wave heights and periods produced different PSDs and that SPM concentration was high further suggest that erosion and flocculation processes, rather than air bubble entrainment, are dominating the observed PSDs.

5.6. Conclusions

Analysis of PSDs together with the interpretation of acoustically and optically derived SPM concentration and altimetry allowed identifying differences in SPM composition during storm conditions. The data show the importance of wind-induced advection, alongshore subtidal flow and HCMS formation as regulating mechanisms of SPM concentration, as well as other SPM characteristics (cohesiveness or composition of sediment particles) and size distribution in a high-turbidity area, rather than solely turbulence shear from currents and waves. The former is the clue to explain the different behaviour of SPM concentrations from ADPs and OBSs and the observed differences in PSDs during different storms. Wind direction and strength influences the subtidal alongshore flow and results in an advection of the coastal turbidity maximum. This is associated with an increase in cohesive SPM concentration, the formation of HCMSs and the armouring of sand during SW storms, or with a decrease in cohesive SPM concentration, no HCMS formation and an increase in sand and silt in suspension during NE storms.

Particle size distributions were generally multimodal and consisting of primary particles, flocculi, microflocs and macroflocs. During NE storms, however, PSDs were unimodal and consisting of mainly granular material (silt, sand) re-suspended from the seabed, whereas during SW storms flocculated material was still being identified in the PSDs. The data suggest that two populations of primary particles ($<3\ \mu\text{m}$ and flocculi $15\ \mu\text{m}$) coexist and are the building blocks of flocs. Flocculi consist of clusters of clay minerals, whereas primary particles are of various compositions (calcite, clays).

Mixed sediments were found in suspension at 2 mab at times of maximum flood currents at spring tide and during storms. At the measurement site, this occurs more prominently when the winds are blowing from the SW-W. The size distribution of the local bed sediments is thus influencing the SPM size distribution only when HCMSs are not present and when turbulence induced by currents (maximum flood currents) or waves is strong enough to bring sand or silt into suspension. Flocs are disappearing from the measurement site when winds are blowing from northerly directions (NW-NE), due to advection.

The study has shown that first estimates of SPM composition can be made using available sensors; the results remain nevertheless qualitative. Detailed analysis of the mineralogical and organic components is, however, necessary to understand SPM dynamics. Quantitative analytical techniques have been developed in the laboratory (Zeelmaekers 2011), but are not available for the collection of in-situ time-series. A new generation of detectors and sensors is needed, based on the different optical and acoustical properties of very heterogeneous SPM components. The study also underlines the necessity of developing common and standardized methodologies for processing acoustic and optical backscatter signals. This is especially needed for sound formulations and interpretations of long-term changes in SPM concentration and composition at a given locality, and in order to meaningfully compare data from different localities collected by emerging coastal and ocean observatories.

5.7. Acknowledgements

The study was partly funded by the Maritime Access Division of the Ministry of the Flemish Community (MOMO project) and by the Belgian Science Policy (Science for a Sustainable Development, QUEST4D, SD/NS/06A). M. Baeye acknowledges a specialisation grant from IWT (Agency for Innovation by Science and Technology, Flanders). B.J. Lee acknowledges financial support from the Flemish Science Foundation (FWO Vlaanderen) for funding the FWO project no. G.0263.08. G. Dumon (Ministry of the Flemish Community, Maritime Services, Coastal Division/Hydrography) made available wind and wave measurement data. We wish to acknowledge the crew of RV Belgica for their skilful mooring and recuperation of the tripod. Measurements would not have been possible without technical assistance of A. Pollentier and his team

(Measuring Service of MUMM, Oostende). The manuscript benefited from the constructive assessments of two anonymous referees.

5.8. References

- Agrawal YC, Pottsmith HC (2000). Instruments for particle size and settling velocity observations in sediment transport. *Marine Geology* 168, 89–114.
- Agrawal YC, Traykovski P (2001). Particles in the bottom boundary layer: concentration and size dynamics through events. *Journal of Geophysical Research* 106(C5), 9533–9542.
- Andrews S, Nover D, Schladow SG (2010). Using laser diffraction data to obtain accurate particle size distributions: the role of particle composition. *Limnology Oceanography: Methods* 8, 5074–526.
- Andrews SW, Nover DM, Reuter JE, Schladow SG (2011). Limitations of laser diffraction for measuring fine particles in oligotrophic systems: pitfalls and potential solutions. *Water Resources Research* 47, W05523.
- Baeye M, Fettweis M, Voulgaris G, Van Lancker V (2011). Sediment mobility in response to tidal and wind-driven flows along the Belgian inner shelf, southern North Sea. *Ocean Dynamics* 61, 611–622.
- Benson T, French JR (2007). InSiPID: a new low-cost instrument for in-situ particle size measurements in estuarine and coastal waters. *Journal of Sea Research* 58, 167–188.
- Berlamont J, Ockenden M, Toorman E, Winterwerp J (1993). The characterisation of cohesive sediment properties. *Coastal Engineering* 21, 105–128.
- Bhaskar PV, Grossart H-P, Bhosle NB, Simon M (2005). Production of macro-aggregates from dissolved exopolymeric substances (EPS) of bacterial and diatom origin. *FEMS Microbiology Ecology* 53, 255–264.
- Bowers DG, Braithwaite KM, Nimmo-Smith WAM, Graham GW (2009). Light scattering by particles suspended in the sea: the role of particle size and density. *Continental Shelf Research* 29, 1748–1755.
- Bunt JAC, Larcombe P, Jago CF (1999). Quantifying the response of optical backscatter devices and transmissometers to variations in suspended particulate matter. *Continental Shelf Research* 19, 1199–1220.
- CEM (2003). *Coastal Engineering Manual*, Chapter 4. Surf zone hydrodynamics. US Army Corps of Engineers, EM 1110-2-1100.
- Chang TS, Flemming B, Bartholomä A (2007). Distinction between sortable silts and aggregated particles in muddy intertidal sediments of the East Frisian Wadden Sea, southern North Sea. *Sedimentary Geology* 202, 453–463.
- Curran KJ, Hill PS, Milligan TG, Mikkelsen OA, Law BA, Durrieu de Madron X, Bourrin F (2007). Settling velocity, effective density, and mass composition of suspended sediment in a coastal bottom boundary layer, Gulf of Lions, France. *Continental Shelf Research* 27, 1408–1421.
- Deane GB, Stokes MD (2002). Scale dependence of bubble creation mechanisms in breaking waves. *Nature* 418, 839–844.
- Downing J (2006). Twenty-five years with OBS sensors: the good, the bad, and the ugly. *Continental Shelf Research* 26, 2299–2318.
- Eisma D (1986). Flocculation and de-flocculation of suspended matter in estuaries. *Netherlands Journal of Sea Research* 20, 183–199.
- Fettweis M (2008) Uncertainty of excess density and settling velocity of mud derived from in-situ measurements. *Estuarine Coastal and Shelf Science* 78, 426–436.
- Fettweis M, Francken F, Pison V, Van den Eynde D (2006). Suspended particulate matter dynamics and aggregate sizes in a high turbidity area. *Marine Geology* 235, 63–74.
- Fettweis M, Francken F, Van den Eynde D, Verwaest T, Janssens J, Van Lancker V (2010). Storm influence on SPM concentrations in a coastal turbidity maximum area with high anthropogenic impact (southern North Sea). *Continental Shelf Research* 30, 1417–1427.
- Forrest J, Clark NR (1989). Characterizing grain size distributions: evaluation of a new approach using multivariate extension of entropy analysis. *Sedimentology* 36, 711–722.

- Fugate DC, Friedrichs CT (2002). Determining concentration and fall velocity of estuarine particle populations using ADV, OBS and LISST. *Continental Shelf Research* 22, 1867–1886.
- Graham GW, Nimmo-Smith WAM (2010). The application of holography to the analysis of size and settling velocity of suspended cohesive sediments. *Limnology and Oceanography: Methods* 8, 1–15.
- Hamilton LJ, Z Shi, SY Zhang (1998). Acoustic backscatter measurements of estuarine suspended cohesive sediment concentration profiles. *Journal of Coastal Research* 14, 1213–1224.
- Hamm CE (2002). Interactive aggregation and sedimentation of diatoms and clay-sized lithogenic material. *Limnology and Oceanography* 47, 1790–1795.
- Hoitink AJF, Hoekstra P (2005). Observations of suspended sediment from ADCP and OBS measurements in a mud-dominated environment. *Coastal Engineering* 52, 103–118.
- Huang SL (1989). The influence of disaggregation methods on X-ray diffraction of clay minerals. *Journal of Sedimentary Research* 59, 997–1001.
- Hussein T, dal Maso M, Petäjä T, Koponen IK, Paatero P, Aalto PP, Hämeri K, Kulmala M (2005). Evaluation of an automatic algorithm for fitting the particle number size distributions. *Boreal Environmental Research* 10, 337–355.
- Johnston RJ, Semple RK (1983). Classification using information statistics. *Concepts and Techniques in Modern Geography* 37. GeoBooks, Norwich.
- Jonasz M, Fournier G (1996). Approximation of the size distribution of marine particles by a sum of log-normal functions. *Limnology and Oceanography* 41, 744–754.
- Kim HY, Gutierrez B, Nelson T, Dumars A, Maza M, Perales H, Voulgaris G (2004). Using the acoustic Doppler current profiler (ADCP) to estimate suspended sediment concentration. University of South Carolina, Columbia (USA), Tech Rep CPSD 04-01.
- Kranenburg C (1994). On the fractal structure of cohesive sediment aggregates. *Estuarine Coastal and Shelf Science* 39, 451–460.
- Krivtsov V, Mikkelsen OA, Jones SE (2011). Entropy analysis of SPM patterns: case study of Liverpool Bay. *Geo-Mar Letter*.
- Lacroix G, Ruddick K, Ozer J, Lancelot C (2004). Modelling the impact of the Scheldt and Rhine/Meuse plumes on the salinity distribution in Belgian waters (southern North Sea). *Journal of Sea Research* 52, 149–163.
- Lee BJ, Toorman E, Molz FJ, Wang J (2011). A two-class population balance equation yielding bimodal flocculation of marine or estuarine sediments. *Water Research* 45, 2131–2145.
- Lick W, Huang H, Jepsen R (1993). Flocculation of fine-grained sediments due to differential settling. *Journal of Geophysical Research* 98, 10279–10288.
- Makela JM, Koponen IK, Aalto P, Kulmala M (2000). One-year data of submicron size modes of tropospheric background aerosol in southern Finland. *Journal of Aerosol Science* 31, 595–611.
- Manning AJ, Bass SJ, Dyer KR (2006). Floc properties in the turbidity maximum of a mesotidal estuary. *Marine Geology* 235, 193–211.
- Manning AJ, Baugh JV, Spearman J, Whitehouse RJS (2010). Flocculation settling characteristics of mud: sand mixtures. *Ocean Dynamics* 60, 237–253.
- Mari X, Burd A (1998). Seasonal size spectra of transparent exopolymeric particles (TEP) in a coastal sea and comparison with those predicted using coagulation theory. *Marine Ecology Progress Series* 163, 63–76.
- Mietta F (2010). Evolution of the floc size distribution of cohesive sediments. PhD Thesis, Delft University of Technology, The Netherlands.
- Mietta F, Chassagne C, Verney R, Winterwerp JC (2010). On the behavior of mud floc size distribution: model calibration and model behavior. *Ocean Dynamics* 61, 257–271.
- Mikkelsen OA, Hill PS, Milligan TG (2006). Single-grain, microfloc and macrofloc volume variations observed with a LISST-100 and a digital floc camera. *Journal of Sea Research* 55, 87–102.
- Mikkelsen OA, Hill PS, Milligan TG (2007) Seasonal and spatial variation of floc size, settling velocity, and density on the inner Adriatic Shelf (Italy). *Continental Shelf Research* 27, 417–430.

- Murphy S, Voulgaris G (2006). Identifying the role of tides, rainfall and seasonality in marsh sedimentation using long-term suspended sediment concentration data. *Marine Geology* 227, 31–50.
- Nechad B, Ruddick KG, Park Y (2010). Calibration and validation of a generic multisensor algorithm for mapping of total suspended matter in turbid waters. *Remote Sensing of Environment* 114, 854–866.
- Orpin AR, Kostylev VE (2006) Towards a statistically valid method of textural sea floor characterization of benthic habitats. *Marine Geology* 225, 209–222.
- Panagiotopoulos I, Voulgaris G, Collins MB (1997). The influence of clay on the threshold of movement of fine sandy beds. *Coastal Engineering* 32, 19–43.
- Pope ND, Widdows J, Brinsley MD (2006). Estimation of bed shear stress using the turbulent kinetic energy approach - A comparison of annular flume and field data. *Continental Shelf Research* 26, 959–970.
- Stewart LK, Kostylev VE, Orpin AR (2009) Windows-based software for optimising entropy-based groupings of textural data. *Computers & Geosciences* 35, 1552–1556.
- Sun D, Bloemendal J, Rea DK, Vandenberghe J, Jiang F, An Z, Su R (2002). Grain-size distribution function of polymodal sediments in hydraulic and aeolian environments, and numerical partitioning of the sedimentary components. *Sedimentary Geology* 152, 263–277.
- Thorne PD, Hanes DM (2002). A review of acoustic measurement of small-scale sediment processes. *Continental Shelf Research* 22, 603–632.
- Thorne PD, Vincent CE, Hardcastle PJ, Rehman S, Pearson ND (1991). Measuring suspended sediment concentrations using acoustic backscatter devices. *Marine Geology* 98, 7–16.
- Thorpe SA (1995). Dynamical processes of transfer at the sea surface. *Progress in Oceanography* 35(4), 315–352.
- van Ledden M, van Kesteren WGM, Winterwerp J (2004). A conceptual framework for the erosion behaviour of sand-mud mixtures. *Continental Shelf Research* 24, 1–11.
- van Leussen W (1994). Estuarine macroflocs and their role in fine-grained sediment transport. PhD Thesis, University Utrecht, The Netherlands.
- Verfaillie E, Van Meirvenne M, Van Lancker V (2006). Multivariate geostatistics for the predictive modelling of the surficial sand distribution in shelf seas. *Continental Shelf Research* 26, 2454–2468.
- Verney R, Lafite R, Brun-Cottan JC, Le Hir P (2011). Behaviour of a floc population during a tidal cycle: laboratory experiments and numerical modelling. *Continental Shelf Research* 31, S64–S83.
- Voulgaris G, Meyers S (2004). Temporal variability of hydrodynamics, sediment concentration and sediment settling velocity in a tidal creek. *Continental Shelf Research* 24, 1659–1683.
- Wallbridge S, Voulgaris G, Tomlinson BN, Collins MB (1999). Initial motion and pivoting characteristics of sand particles in uniform and heterogeneous beds: experiments and modeling. *Sedimentology* 46, 17–32.
- Whitby K (1978). The physical characteristics of sulfur aerosols. *Atmospheric Environment* 41, S25–S49.
- Wiberg PL, Drake DE, Cacchione DA (1994). Sediment re-suspension and bed armoring during high bottom stress events on the northern California inner continental shelf: measurements and predictions. *Continental Shelf Research* 14, 1191–1219.
- Williamson H, Torfs H (1996). Erosion of mud/sand mixtures. *Coastal Engineering* 29, 1–25.
- Winter C, Katoshevski D, Bartholomä A, Flemming BW (2007). Grouping dynamics of suspended matter in tidal channels. *Journal of Geophysical Research* 112, C08010.
- Winterwerp JC (1998). A simple model for turbulence induced flocculation of cohesive sediment. *Journal of Hydraulic Research* 36, 309–326.
- Woolfe KJ, Michibayashi K (1995). "Basic" entropy grouping of laser-derived grain-size data: an example from the Great Barrier Reef. *Computers & Geosciences* 21, 447–462.

- Woolfe KJ, Fielding CR, Howe JA, Lavelle M, Lally JH (1998). Laser-derived particle size characterisation of CRP-1, McMurdo Sound, Antarctica. *Terra Antarctica* 5, 383–391.
- Wu B, Molinas A, Shu A (2003). Fractional transport of sediment mixtures. *International Journal of Sedimentary Research* 18, 232–247.
- Zeelmaekers E (2011). Computerized qualitative and quantitative clay mineralogy – Introduction and application to known geological cases. PhD Thesis, Katholieke Universiteit Leuven, Belgium. ISBN 978-90-8649-414-9. XII, 397 pp.